High-Resolution Brillouin Scattering

E. I. GORDON AND M. G. COHEN
Bell Telephone Laboratories, Murray Hill, New Jersey
(Received 19 August 1966)

A new technique for determining the velocity and attenuation of hypersound is established. Experiments illustrating the technique with water as the acoustic medium in the frequency range 500–1500 Mc/sec are described. The technique is based on superheterodyne detection of Brillouin-scattered light from a multifrequency gas laser. The scattering sound is injected from a buffer rod into the medium under study, in contrast to the classic Brillouin-scattering technique, which uses scattering from ubiquitous thermal phonons, and detects by means of photon counting. Measurement of the amplitude and phase of the microwave photocurrent (using a homodyne technique) as a function of the angle of the buffer rod determines the attenuation constant and phase velocity of the hypersound. The technique is especially useful at those hypersonic frequencies for which the attenuation is sufficiently great that the pulse-echo technique or other acoustic reflection techniques are difficult or impossible and yet small enough that the classic Brillouin-scattering technique has insufficient resolution. The experiments in water described here correspond to such a range, and bridge the gap between the available ultrasonic data and more recent measurements above 3 Gc/sec. In particular, the data indicate that for water an upper limit of 10^{-11} sec can be set for the relaxation time associated with excess loss.

INTRODUCTION

THE classic Brillouin-scattering technique has experienced a brisk renewal of interest as laser light sources have become available. Benedek and Greytak have reviewed the history and theory of the subject and recent measurements.[1] The classic technique utilizes the light scattered by thermally produced phonons; at any given angle relative to the direction of the incident light, the light scattered by phonons of a given wavelength contains a doublet split in frequency symmetrically relative to the frequency of the incident light. The splitting and spectral width of the individual components of the doublet, coupled with knowledge of the optical wavelength and required acoustic wavelength for scattering, yield the velocity and lifetime or decay rate of the scattering phonons. The accuracy and resolution is limited, however, by the requisite optical spectrometer or interferometer and the multifrequency character of laser sources. Even with single-frequency gas lasers,[1] the optical resolution is limited to several tens of megacycles per second.

Utilizing injected phonons of a well-defined frequency, Cohen and Gordon[2] have demonstrated a new scattering technique based on measurement of the angular spread of the scattered light. The phonon decay and consequent spread in phonon momentum introduces a spread in the direction of the scattered light with an angular width inversely proportional to the phonon decay distance. The center angle of the scattered light measures the acoustic velocity. The accuracy and resolution is considerably greater than that of the classic experiment. Furthermore, attenuation and velocity are determined as a function of phonon energy or frequency rather than as a function of phonon wavelength as in the classical technique. When dispersion is present, the difference is nontrivial and the new measurement technique may be more fundamental.

Nevertheless, when the acoustic frequency is high so that the decay distance is very short, the need to bring the light beam very close to the acoustic source makes an alternative but closely related technique desirable. The purpose of this paper is to establish the theoretical basis for the alternative technique and to describe an experiment in water in the range 500–1500 Mc/sec illustrating its validity and usefulness.

DESCRIPTION OF THE EXPERIMENTAL TECHNIQUE

Consider the geometry shown in Fig. 1. A narrow acoustic beam of angular frequency Ω is transmitted into a liquid medium normal to the optically flat face of the buffer rod. The transducer geometry is chosen so that the beam waist of width L occurs approximately at the interface with the liquid medium with a width

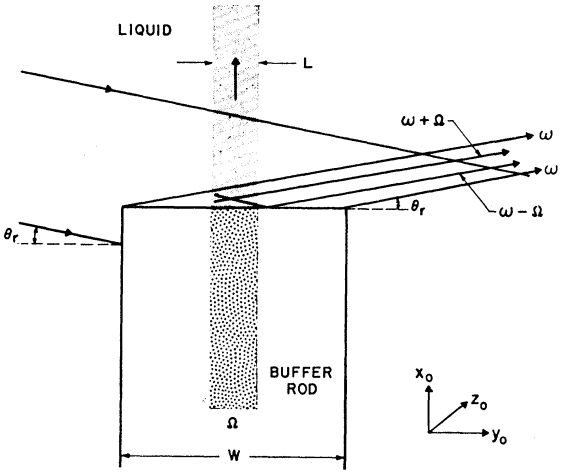

FIG. 1. Scattered beams at $\omega+\Omega$ and $\omega-\Omega$ traveling approximately collinear with specularly reflected beam at ω.

[1] G. Benedek and T. Greytak, Proc. IEEE 53, 1623 (1965).
[2] M. G. Cohen and E. I. Gordon, Bell System. Tech. J. 44, 693 (1965).

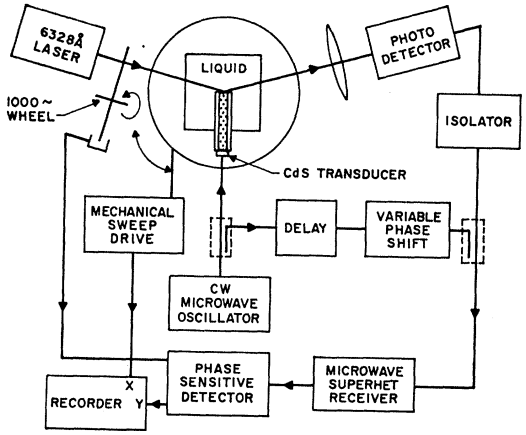

FIG. 2. Block diagram of experimental arrangement.

small compared to the width of the rod. A wide, parallel light beam chopped at 1000 cps is incident on the face of the rod at an angle corresponding approximately to the Bragg angle appropriate to the acoustic frequency. The incident light beam may contain a small range of frequencies, but for the purpose of discussion consider only the component at some frequency ω. The light beam is specularly reflected off the face of the buffer rod. Approximately colinear with the reflected beam are two components of scattered light, one at frequency $\omega+\Omega$ arising from acoustic scattering of the incident light beam, a second at frequency $\omega-\Omega$ arising from scattering of the specularly reflected beam. After undergoing specular reflection, the direction of the $\omega-\Omega$ component is parallel to the $\omega+\Omega$ component; however, its amplitude is reduced relative to that of the $\omega+\Omega$ component by two specular reflections from the face of the rod.

The light scattered into the angular range occupied by the specularly reflected beam is superheterodyne detected with a square-law photodetector using the specularly reflected beam as the local oscillator. As shown in Fig. 2, the microwave output of the photodetector at frequency Ω is homodyne detected using the cw input signal to the transducer as the reference.[3] Each frequency component of the incident light beam contributes coherently and in-phase to the signal at Ω. All other components of the photocurrent not coherent with the injected signal are reduced in amplitude relative to the signal at Ω; the larger the injected signal the larger the relative reduction.[3] The video output of the microwave receiver, which has a chopped component, is phase-sensitive detected using the 1000 cps signal from the chopping wheel as the reference. A typical video signal is shown in Fig. 3; the dc level corresponds to the injected signal while the square-wave component corresponds to the coherent addition or subtraction of the photocurrent. The two photographs correspond to relative phase of π or zero.

The angular spread of the scattered light is determined by observing the amplitude of the video signal while rocking the buffer rod slowly through an angular range centered about the Bragg angle. A reference voltage proportional to the angular sweep is applied to the x axis of the recorder and the output of the phase-sensitive detector is applied to the y axis. The recorded signal is proportional to the amplitude and phase of the photodetector current at Ω as a function of the angle of the buffer rod, which yields the attenuation and velocity of the acoustic wave as derived in Appendix A and summarized in what follows: The pertinent result for the photocurrent at angular frequency Ω is

$$\iota(\Omega)=\iota_0\frac{\exp[i\Omega(t-R/c')]}{\beta(1+\eta^2)}\times[1-(\exp(-\beta))(\cos\beta\eta-\eta\sin\beta\eta)+i[\eta-(\exp(-\beta))(\sin\beta\eta+\eta\cos\beta\eta)]], \quad (1)$$

in which the angle parameter η is given by

$$\eta=2(k/\alpha)[\sin\theta_r-\sin\Theta], \quad (2)$$

θ_r being the nominal angle of the reflected- or incident-light beam relative to the face of the rod, Θ the Bragg angle, k the propagation constant of the light within the medium, and 2α the decay constant for the acoustic energy. The decay time or lifetime of the phonon is given by $(2\alpha v)^{-1}$, v being the acoustic velocity. The constant ι_0 is related to the power of the reflected light and amplitude of the sound as well as the reflectivity of the buffer rod and will be discussed later. The parameter

$$\beta=\tfrac{1}{2}\alpha W\tan\theta_r \quad (3)$$

is (within a factor π^{-1}) the ratio of the Lorentzian diffraction half-width of the scattered light to the $(\sin X/X)^2$ diffraction half-width of the light reflected off the face of the rod; W is the width of the rod. With proper design of the experiment, $\beta\gg1$ and the microwave photocurrent takes the simpler form[4]

$$\iota(\Omega)=\iota_0\beta^{-1}\exp[i\Omega(t-R/c')]\left[\frac{1+i\eta}{1+\eta^2}\right]. \quad (4)$$

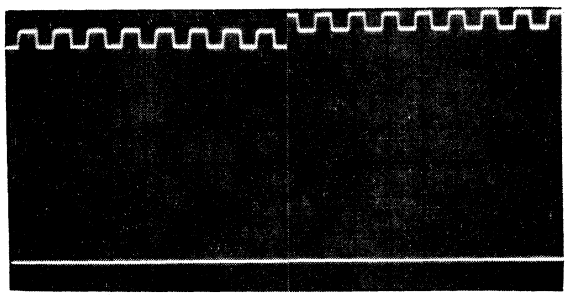

FIG. 3. Video output of superheterodyne receiver for $\varphi=\pi$ (left) and $\varphi=0$ (right).

[3] M. G. Cohen and E. I. Gordon, Bell System Tech. J. 42, 3068 (1964).

[4] Equation (1), which leads to (4) under the condition $\frac{1}{2}\alpha W\tan\theta_r\gg1$, is valid under the restriction $\frac{1}{2}\alpha L\tan\theta_r\ll1$, i.e., a narrow acoustic beam. In Appendix A it is shown that (4) is valid under the more general restriction $\frac{1}{2}\alpha(W-L)\tan\theta_r\gg1$.

With the arrangement shown in Fig. 2, setting the injected microwave current level at Ω large compared to the microwave photodetector current and operating the mixer and i.f. detector as linear envelope detectors, the chopped video output voltage of the microwave superheterodyne receiver is[3]

$$V \propto \mathrm{Re}\left[\frac{1+i\eta}{1+\eta^2}\exp i\varphi\right]=\left[\frac{1}{1+\eta^2}\right]\cos\varphi-\left[\frac{\eta}{1+\eta^2}\right]\sin\varphi, \quad (5)$$

in which φ is the phase of the injected microwave current relative to that from the photodetector. The integrated output of the phase-sensitive detector is proportional to V. Consequently, when $\varphi=0$ or π the experimental curve should be Lorentzian, $[1+\eta^2]^{-1}$, and for $\varphi=\pm\pi/2$ it should be of the dispersion form $\eta/(1+\eta^2)$. For either curve the values $\eta=\pm1$, as determined from the half-power points of the Lorentzian or the maxima of the dispersion curve, yield the angular width

$$\Delta\theta_r=\alpha/(k\cos\Theta), \quad (6)$$

as follows from (2). Measurement of $\Delta\theta_r$ determines α. The value $\eta=0$ corresponds to

$$\sin\theta_r=\sin\Theta=\tfrac{1}{2}\Omega/kv, \quad (7)$$

which measures the phonon velocity.

Before proceeding with a description of the experiment, it might be appropriate to provide some physical insight into the basis for this result. Consider Fig. 4, which shows schematically the incident-light photon with momentum $\hbar k$ directed along a—a′, as well as the reflected photon directed along b—b′. The reflecting surface of the rod has its normal along c—c′, which is also the direction of the injected phonons, ignoring acoustic diffraction. Only the component of scattered light collinear with the reflected beam produces a beat in the photodetector. In addition, the momentum of the scattered photon is but trivially changed from that of the incident photon, since its energy differs by at most a few parts in 10^5. Hence, only that component of the phonon momentum which satisfies momentum conservation relative to the incident and reflected photon can contribute to the beat signal. Consequently, as the angle θ_r is scanned by varying the direction of c—c′ (which automatically varies the direction b—b′ as well as the direction of the phonon momentum), the amplitude of the beat measures the amplitude distribution of phonon momentum. Since the acoustic energy decays exponentially, the distribution of phonon momentum is Lorentzian, with a width proportional to the decay rate. Hence, the amplitude distribution at constant phase is also Lorentzian as indicated by (5).

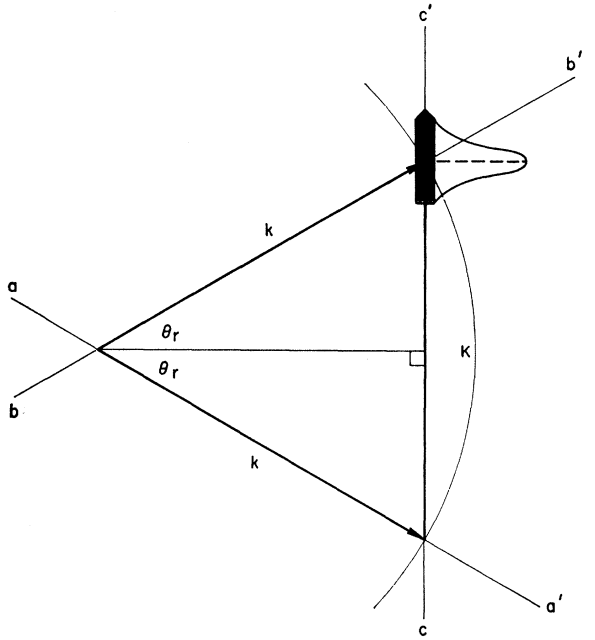

FIG. 4. Scattering interaction with Lorentzian distribution of phonon momentum; $\hbar K$ is the phonon momentum.

EXPERIMENT

The experiment was performed in water in the range 500–1500 Mc/sec. This choice was dictated by the following considerations. At 1000 Mc/sec, the phonon decay distance is about 2.5×10^{-3} cm, so that pulse-echo techniques are extremely difficult. On the other hand, the linewidth for the classic scattering experiment is expected to be about 10 Mc/sec, too low for the available resolution of that technique. Consequently, it has not been possible to study water accurately in this range of hypersonic frequencies. Similar limitations hold for other liquids and solids. Furthermore, the parameter $\beta=\frac{1}{2}\alpha W\tan\Theta$[5] varies approximately as f^3 (f is the hypersonic frequency of measurement), since $\alpha\propto f^2$ and $\tan\Theta\propto f$. Consequently, for the single buffer rod and CdS evaporated film transducer used in the range 500–1500 Mc/sec, β varied over a range of 30:1 and it was possible to study the case $\beta\approx1$ as well as $\beta\gg1$. While $\beta\approx1$ represents limiting resolution and is not experimentally interesting, understanding and observing this limit lends additional credence to the measurement technique. For the case β not necessarily large, (5) takes the form

$$V\propto\left[\frac{1-(\exp-\beta)(\cos\beta\eta-\eta\sin\beta\eta)}{1+\eta^2}\right]\cos\varphi-\left[\frac{\eta-(\exp-\beta)(\sin\beta\eta+\eta\cos\beta\eta)}{1+\eta^2}\right]\sin\varphi, \quad (8)$$

as follows from (1). This form can be considered to be the convolution of the $(\sin X/X)$ distribution of the reference beam and the Lorentzian distribution of the scattered light. Figure 5 illustrates the in-phase compo-

[5] Since $\theta_r\approx\Theta$ throughout any given angular scan, $\tan\theta_r$ can be approximated by $\tan\Theta$ with negligible error.

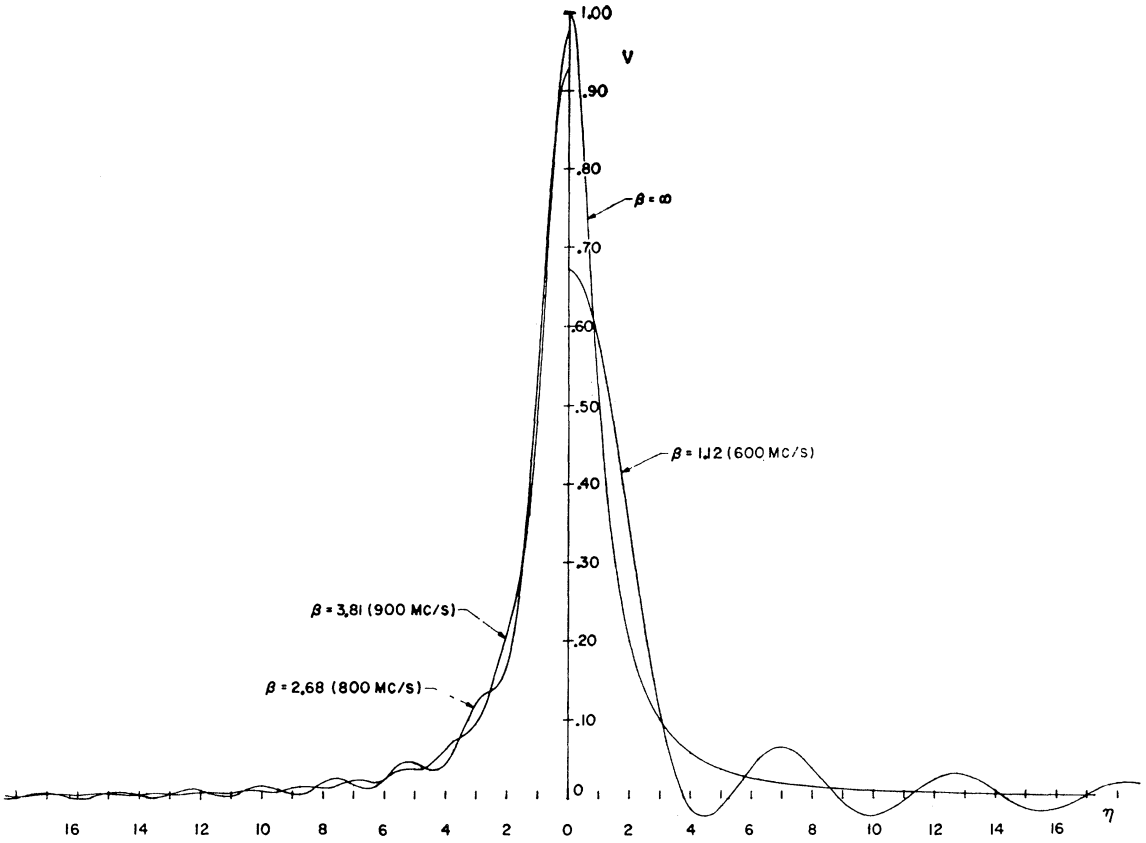

FIG. 5. Amplitude of beat signal V for $\varphi=0$ and $\beta=1.12$, 2.68, 3.81, and ∞.

nent for several values of β. Note that $\beta=3.81$ is virtually indistinguishable from $\beta=\infty$.

The experimental arrangement illustrated in Fig. 2 very closely summarizes the experimental configuration, but several aspects require further elaboration. The use of a long quartz buffer rod is advantageous at hypersonic frequencies in that acoustic resonances and hence frequency sensitivity are inhibited by the associated loss. On the other hand, the long delay (4 μsec) makes the phase of the acoustic signal injected into the water critically dependent upon acoustic frequency. In fact, a frequency change of 60 kc/sec changes the phase by $\pi/2$. Consequently, extreme frequency stability ($\sim$1 kc/sec) or a compensating delay in the homodyne signal arm is required. The use of a shorter, lossier rod would work, but would limit the experimental range. In the experiments described here, the frequency stability of the oscillator was just adequate and no compensation was used.

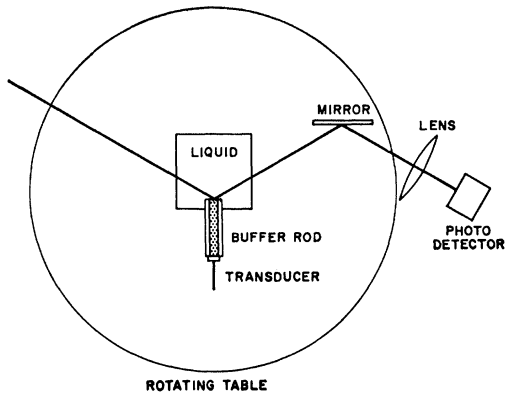

FIG. 6. Scattering cell with additonal mirror on rotating table.

As indicated in Appendix A, it is necessary that the width of the acoustic beam L be chosen such that $(1-L/W)\beta=\frac{1}{2}\alpha(W-L)\tan\Theta\gg1$. For the experiments described here, $W=3.18$ mm and $L\approx\frac{1}{4}W$, which yields the value $\beta\approx3.81$ at 900 Mc/sec.

In Appendix A, it is shown that the amplitude of the beat signal is proportional to the quantity $\Gamma(1-|\Gamma|^2)$ in which $|\Gamma|^2$ is the reflectivity of the liquid–buffer rod interface. This results from the fact that the beat signal arising from the scattered light at $\omega+\Omega$ is π out of phase with the signal arising from the light at $\omega-\Omega$. A very broad maximum exists at $|\Gamma|^2=\frac{1}{3}$. It can be shown that for light polarized with the E field perpendicular to the plane of incidence and incident at the Bragg angle,

$$|\Gamma|^2=\left[\frac{[n_2^2-n_1^2+(\frac{1}{2}f\lambda_0/v)^2]^{1/2}-\frac{1}{2}f\lambda_0/v}{[n_2^2-n_1^2+(\frac{1}{2}f\lambda_0/v)^2]^{1/2}+\frac{1}{2}f\lambda_0/v}\right]^2, \quad (9)$$

in which f is the acoustic frequency, λ_0 the free-space wavelength of the light, and n_1 and n_2 the indices of refraction of the water and quartz, respectively. The reflectivity varies from 0.53 at 500 Mc/sec to 0.29 at

1000 Mc/sec to 0.16 at 1500 Mc/sec; consequently, $\Gamma(1-|\Gamma|^2)$ is greater than 85% of its maximum value throughout the range.

The He-Ne laser at 0.6328 μ provided a multifrequency power of 8 mW in the lowest order transverse mode. Only a small portion of the beam center was reflected from the face of the rod. The reflected power was several hundred microwatts and a silicon microwave photodiode (TI-LSX900) provided shot-noise limited photosensitivity. In order to keep the reflected beam focused on the same area of the photodetector as the angle θ_r was varied, an additional mirror fixed to the rotating table was used as shown in Fig. 6. It should be noted that refraction at the air-liquid cell interface requires the proper interpretation of θ_r relative to the angle of the table θ_r'. However, when the cell interface is approximately parallel to the buffer rod, θ_r can be interpreted as the external angle θ_r' if k is set equal to the propagation constant in air, $2\pi/\lambda_0$.

Figure 7 shows typical tracings obtained for $f=1200$ Mc/sec using an integration time of 0.1 sec in the phase-sensitive detector. The plotted points are the expected curves $(1+\eta^2)^{-1}$ and $\eta(1+\eta^2)^{-1}$ matched to the data at $\eta=0$ and ±1. Figure 8 illustrates data obtained at $f=600$ Mc/sec corresponding to $\beta=1.12$, which should be compared to Fig. 5. In summary, the agreement for frequencies at 900 Mc/sec and above is essentially perfect. Below 900 Mc/sec, the agreement is qualitatively very good. It should be noted that measurements of the far-field distribution of the specularly reflected beam indicate that the angular distribution is almost, but not quite, $(\sin X/X)^2$, and this can account for lack of perfect agreement when the angular width of the scattered light is comparable to that of the reflected light. Figure 9 presents the measured values of α at 23°C. The solid line summarizes the ultrasonic data[6] and the one point at 250 Mc/sec was obtained from Ref. 2. The measurement accuracy is believed to be within $\pm1\%$. The scatter in the data is consistent with variation in the water temperature which corresponded to ambient room temperature.

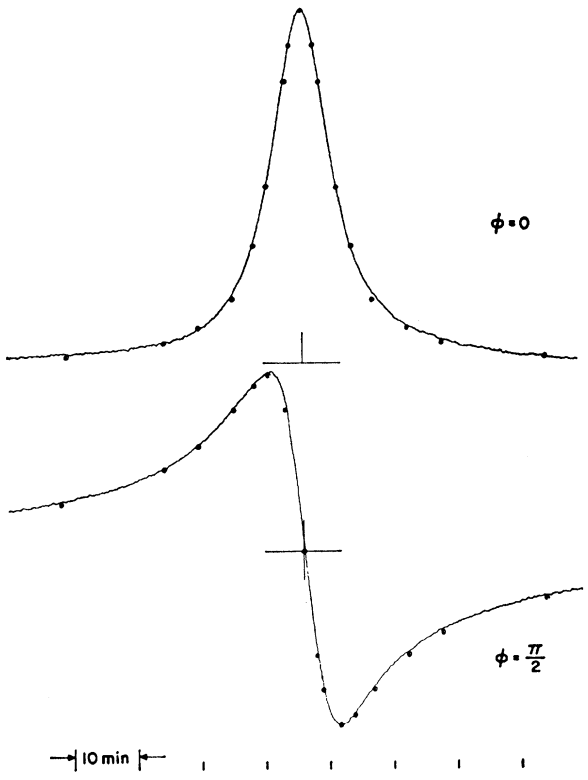

FIG. 7. Output of phase-sensitive detector for $f=1200$ Mc/sec. The plotted points are (5) for $\varphi=0$ and $\varphi=\pi/2$ matched to the data at $\eta=0$, and ±1.

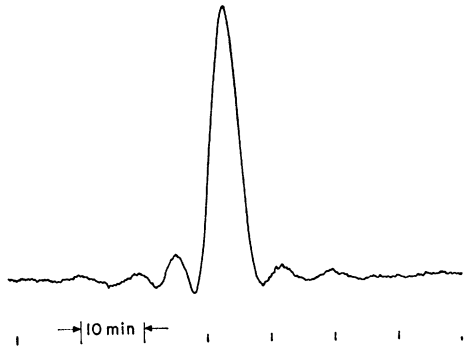

FIG. 8. Output of phase-sensitive detector for $f=600$ Mc/sec for comparison with Fig. 5, $\beta=1.12$.

If the excess absorption in water can be attributed to a single relaxation process, then at 23°C

$$\alpha/f^2=21.5\{0.32+0.68/[1+(2\pi f)^2\tau^2]\}\times10^{-17}(\text{cm}^{-1}\,\text{sec}^2), \quad (10)$$

in which the first term in the bracket corresponds to the classical loss and the second term to the excess loss.[6]

Following Herzfeld and Litovitz,[6] one can predict a value $\tau=2.2\times10^{-12}$ sec, using the theory of Hall,[7] and $\tau=4.4\times10^{-11}$, using the theory of Euken.[8] Relaxation would produce an unobservable decrease in α/f^2 at 1500 Mc/sec using Hall's τ, but a 10% decrease using Euken's value, which is apparently too large. A similar conclusion has been reached by Fleury and Chiao[9] on the basis of a lack of observed velocity dispersion in the 3–6 Gc/sec range. The measured value of v using (9) was found to be $(1.490\pm0.005)\times10^5$ cm/sec, which is also in agreement with Fleury and Chiao.

CONCLUSION

A new technique for measuring acoustic attenuation and velocity in transparent materials has been de-

[6] K. F. Herzfeld and T. A. Litovitz, *Absorption and Dispersion of Ultrasonic Waves* (Academic Press Inc., New York, 1959).
[7] L. Hall, Phys. Rev. **73**, 772 (1948).
[8] A. Eucken, Z. Elektrochem. **52**, 255 (1948).
[9] P. A. Fleury and R. Y. Chiao, J. Acoust. Soc. Am. **39**, 715 (1966).

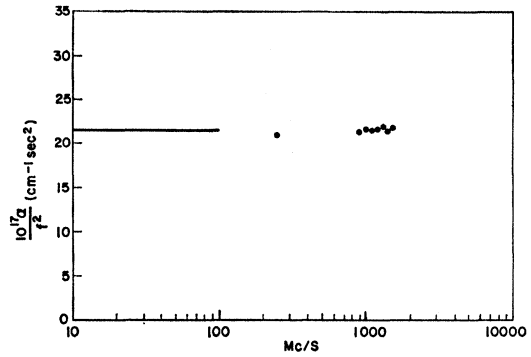

FIG. 9. Absorption coefficient α plotted as $10^{17}\,\alpha/f^2$ versus f at 23°C. The solid line summarizes the ultrasonic data, the point at 250 Mc/sec was taken from Ref. 2, and the experimental results of this work are presented for 900–1500 Mc/sec.

scribed. This technique is useful in those frequency ranges for which purely ultrasonic techniques such as pulse echo or measurements of the complex acoustic impedance by reflection[10] are extremely difficult or impossible and classical Brillouin-scattering techniques have insufficient resolution. Measurements in water in the range 500–1500 Mc/sec indicate that the relaxation time associated with excess loss is $\lesssim 10^{-11}$ sec.

Note added in proof. Recently, M. A. Woolf, P. M. Platzman, and M. G. Cohen [Phys. Rev. Letters **17**, 294 (1966)], have reported on the use of this new technique for measurements in liquid helium II.

ACKNOWLEDGMENTS

The authors are grateful to M. A. Woolf for encouragement and useful discussion throughout the course of the work. Without his stimulus, the initial conception would have remained just another idea. The evaporated CdS film transducer was made by N. F. Foster.

APPENDIX A: CALCULATION OF THE PHOTOCURRENT $\imath(\Omega)$

Experimentally, the photodectector is placed in the focal plane of a lens which collects all the scattered and reflected light. Hence, for the purpose of calculation, the photosurface may be assumed to lie on the surface of a hemisphere of radius R, sufficiently large that far-field approximations are valid. Under steady-state conditions, assuming a time variation $\exp i\omega t$, the reflected wave amplitude (referring to Fig. 1) may be calculated from the scalar Green's-function solution,[11]

$$\psi_{r,\omega}(X,Y,Z)=\frac{1}{4\pi}\oint[G_k(\mathbf{r}|\mathbf{r}_0)\mathrm{grad}_0\psi_r(\mathbf{r}_0) -\psi_r(\mathbf{r}_0)\mathrm{grad}_0 G_k(\mathbf{r}|\mathbf{r}_0)]\cdot d\mathbf{A}_0, \quad \text{(A1)}$$

in which the choice

$$G_k(\mathbf{r}/\mathbf{r}_0)=\frac{\exp(-ik|\mathbf{r}-\mathbf{r}_0|)}{|\mathbf{r}-\mathbf{r}_0|}$$

corresponds to an outgoing wave solution. The observation point is at

$$X=R\cos\varphi\sin\theta,$$
$$Y=R\cos\varphi\cos\theta,$$
$$Z=R\sin\varphi,$$

$$|\mathbf{r}-\mathbf{r}_0|\approx R-x_0\cos\varphi\sin\theta-y_0\cos\varphi\cos\theta-z_0\sin\varphi,$$

and

$$\psi_r(\mathbf{r}_0)=\Gamma\psi_i\exp[-ik(x_0\sin\theta_r+y_0\cos\theta_r)]$$

is the amplitude of the reflected wave at the buffer-rod face (Γ is the amplitude reflectivity) when ψ_i is the amplitude of the incident wave. For this geometry,

$$d\mathbf{A}\cdot\mathrm{grad}_0=-dy_0dz_0\partial(\ )/\partial x_0. \quad \text{(A2)}$$

Taking W equal to the width of the rod, $-\frac{1}{2}W\leq y_0\leq\frac{1}{2}W$ and H its height, $-\frac{1}{2}H\leq z_0\leq\frac{1}{2}H$, yields

$$\psi_{r,\omega}(X,Y,Z)=\frac{ik\Gamma\psi_i WH}{4\pi R}[\exp(-ikR)](\sin\theta_r+\sin\theta\cos\varphi)\times\left[\frac{\sin\frac{1}{2}kW(\cos\theta_r-\cos\theta\cos\varphi)}{\frac{1}{2}kW(\cos\theta_r-\cos\theta\cos\varphi)}\right]\left[\frac{\sin\frac{1}{2}kH\sin\varphi}{\frac{1}{2}kH\sin\varphi}\right].$$

Similarly, the scattered wave at frequency $\omega+\Omega$ may be determined from the volume Green's-function solution[11]

$$\psi_{s,\omega+\Omega}(X,Y,Z)=\int\int\int\rho G_{k'}dv_0, \quad \text{(A3)}$$

in which ρ is the component of volume polarization at frequency $\omega+\Omega$ and $k'=k(1+\Omega/\omega)\approx k$. The volume polarization is proportional to the product of the incident-wave amplitude and the acoustic strain. Absorbing the proportionality constant into the acoustic-strain amplitude S_0, ρ may be written

$$\rho=\{\psi_i\exp[-ik(-x_0\sin\theta_r+y_0\cos\theta_r)]\}\times\{S_0\exp[-(\alpha+iK)x_0]\},$$

in which K is the acoustic-propagation constant Ω/v and α the amplitude-attenuation constant. Substituting into (A3) and performing the integration, assuming the acoustic beam has a width L and height h, ($-\frac{1}{2}L\leq y_0\leq\frac{1}{2}L$, $-\frac{1}{2}h\leq z_0\leq\frac{1}{2}h$, and $0\leq x_0<\infty$), yields

$$\psi_{s,\omega+\Omega}(X,Y,Z)=\left(\frac{hL}{\alpha R}\right)\psi_i S_0[\exp(-ik'R)]\times\left[\frac{\sin\frac{1}{2}kh\sin\varphi}{\frac{1}{2}kh\sin\varphi}\right]\left[\frac{\sin\frac{1}{2}kL(\cos\theta\cos\varphi-\cos\theta_r)}{\frac{1}{2}kL(\cos\theta\cos\varphi-\cos\theta_r)}\right]\times\frac{1}{1-i(k\sin\theta\cos\varphi+k\sin\theta_r-K)/\alpha}. \quad \text{(A4)}$$

[10] J. Lamb and H. Seguin, J. Acoust. Soc. Am. **39**, 519 (1966).
[11] P. M. Morse and H. Feshbach, *Methods of Theoretical Physics* (McGraw-Hill Book Company, Inc., New York, 1953), Sec. 7.2.

The differential photocurrent per unit area on the photodetector surface is proportional to $\psi^*_{r,\omega}\psi_{s,\omega+\Omega}$, hence the total photocurrent may be written

$$\iota(\Omega) \propto (\exp i\Omega t)R^2 \int_0^{\pi/2} \cos\theta d\theta \int_{-\pi}^{+\pi} \psi^*_{r,\omega}\psi_{s,\omega+\Omega} d\varphi . \quad \text{(A5)}$$

Noting that the integrand is sharply peaked at $\varphi=0$ because $kh\gg 1$ and $kH\gg 1$, the φ integral may be integrated in straightforward fashion taking $\cos\varphi=1$ wherever it appears. Since $kL\gg 1$ and $kW\gg 1$, the integrand is also sharply peaked about $\theta=\theta_r$. Defining

$$\xi=\tfrac{1}{2}kW(\cos\theta-\cos\theta_r)\approx -\tfrac{1}{2}kW\ \sin\theta_r(\theta-\theta_r),$$

(A5) becomes

$$\iota(\Omega) \propto -i\Gamma^*|\psi_i|^2 S_0(HL/\alpha) \times\cos\theta_r \exp[i\Omega(t-R/c')]I, \quad \text{(A6)}$$

in which c' is the light velocity and

$$I=\int_{-\infty}^{+\infty} d\xi \left(\frac{\sin\xi}{\xi}\right)\left(\frac{\sin a\xi}{a\xi}\right)\frac{1}{1-i\eta-i\xi/\beta}, \quad \text{(A7)}$$

in which

$$a=L/W,$$
$$\beta=\tfrac{1}{2}\alpha W\ \tan\theta_r,$$
$$\eta=(2k/\alpha)(\sin\theta_r-\sin\Theta),$$
$$\sin\Theta=\tfrac{1}{2}K/k.$$

The integral I can be shown by appropriate contour integration in the complex plane to have the value

$$I=\frac{\pi}{1-i\eta}\left[1-\frac{\exp[-(1-a)\beta(1-i\eta)]-\exp[-(1+a)\beta(1-i\eta)]}{2a\beta(1-i\eta)}\right]. \quad \text{(A8)}$$

Since the reflected optical power can be written

$$P_{\text{optical}} \propto |\psi_i|^2 HW\ \sin\theta_r$$

and the acoustic power can be written

$$P_{\text{acoustic}} \propto |S_0|^2 Lh,$$

(A6) can be written

$$\iota(\Omega) \propto i\Gamma^* P_{\text{optical}} P^{1/2}{}_{\text{acoustic}} (L/h)^{1/2}\beta^{-1} I \times\exp[i\Omega(t-R/c')]. \quad \text{(A9)}$$

The photocurrent arising from the scattered component at $\omega-\Omega$ differs only in that the factor $i\Gamma^*$ is replaced by $-i\Gamma^*|\Gamma|^2$ because of two additional reflections, hence

$$\iota(\Omega)=\iota_0 \exp[i\Omega(t-R/c')]\beta^{-1}I/\pi, \quad \text{(A10)}$$

in which

$$\iota_0 \propto \Gamma^*(1-|\Gamma|^2)P_{\text{optical}} P^{1/2}{}_{\text{acoustic}} (L/h)^{1/2}.$$

When $a\beta=\tfrac{1}{2}\alpha L\ \tan\theta_r \ll 1$, I has the form

$$I\approx\frac{\pi}{1-i\eta}\{1-\exp[-\beta(1-i\eta)]\}$$

and (A10) reduces to the form given in (1). When

$$(1-a)\beta=\tfrac{1}{2}\alpha(W-L)\tan\theta_r\gg 1, \quad \text{(A11)}$$

(A8) reduces to

$$I\approx\frac{\pi}{1-i\eta}$$

and (A10) takes the form given in (4).

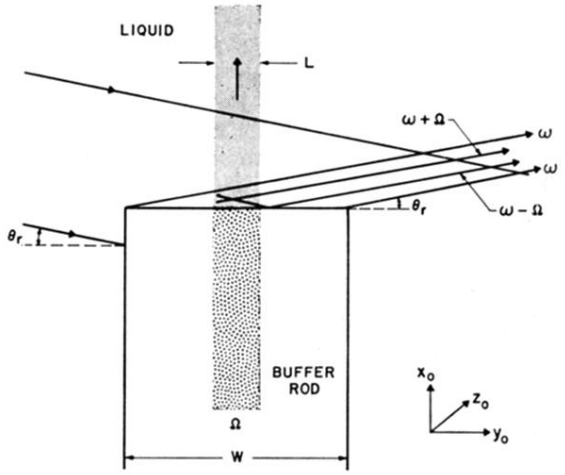

FIG. 1. Scattered beams at $\omega+\Omega$ and $\omega-\Omega$ traveling approximately collinear with specularly reflected beam at ω.

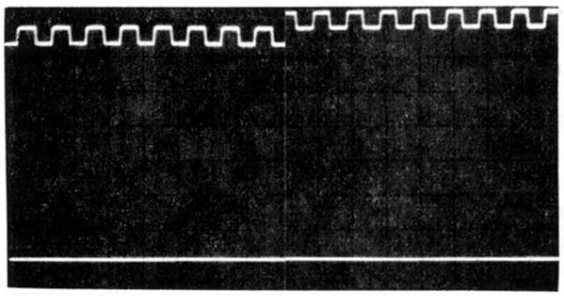

FIG. 3. Video output of superheterodyne receiver for $\varphi=\pi$ (left) and $\varphi=0$ (right).